BABEŞ-BOLYAI UNIVERITY

CLUJ – NAPOCA

PHYSICS FACULTY

SYNTHESIS AND CHARACTERIZATION OF STRUCTURAL, ELECTRIC AND MECHANICAL PROPERTIES OF POLYCRYSTALLINE SUPERCONDUCTORS BI:2223

PhD Thesis Summary

Scientific supervisor :

Prof. Dr. Pop Aurel

PhD Student :

Coldea Roxana

Cluj-Napoca

2011

Contents

Keywords:

Bi2223 bulk HTS, different sintering conditions, X-ray diffraction, electric resistance, Vickers micro hardness, AC susceptibility measurements

Introduction

Superconductivity of metals was discovered in 1911 by Kammerling Onnes, but the most important step in the history of superconducting materials was made in 1986 when high temperature superconductivity (HTS) was discovered in oxidic materials. In the science community this was a very important moment and a huge group of researchers has been oriented to study the superconductor materials. [1,2]

A lot of trials have been made to synthesize new HTS materials by the critical transition temperature close to the room temperature. Unfortunately since now they have not found such material.

Many efforts were made to study the structural, electric, magnetic and optically properties of superconducting materials in order to explain superconductivity at high temperature.

In this PhD thesis I studied the structural, electric and magnetic properties of some polycrystalline superconducting materials (Bi,Pb):2223.

This work begins with an overview of superconductivity and presents the most important characteristics of superconductors, which make them different from other materials.

Chapter three presents different sintering methods for bulk superconductors, and chapter four shows some experimental methods for study bulk materials.

Chapter 5 is devoted to experimental procedures we used to obtain and characterize the superconducting samples and study how their properties change depending on the sintering condition.

In chapter six we investigate the effect of partial atomic substitution of Cu by 3d elements in (Bi,Pb):2223 superconductor on electrical and magnetic properties of this compounds.

1. Supreconductors – general aspects

The theoretical understanding of superconductivity is extremely complicated. The superconductors have the property to carrying the electrical current without any energy losses. Superconductivity at high temperature is probably the most study phenomena due to future possible application.

The basic properties of superconducting materials are:

- zero resistivity below critical temperature Tc [3]
- the exclusion of magnetic field (Meissner effect) and ideal diamagnetism for H<HC [4]

Superconductors have three fundametal characteristics:

- Critical temperature, Tc - represents the value of temperature where the material becomes superconductor, for T<Tc we have zero rezistivity

- Critical magnetic field, Hc - represents the field value over we have the superconductor to normal state transitions

- Critical current, Ic, - correlated with electrical conductivity and Meissner effect. The limit value of electric current through a material which still retains the properties of superconducting material is called critical current.

2. Synthesis methods of polycrystalline bulk superconductors

Any method for polycrystalline compound preparation has direct fundament a phase diagram which delivers the information about obtaining modalities of that compound. In case of Bi2Sr2Ca2Cu3O10 compound, it exist many methods used for his synthesis. From technological point of view, the most important aspect is compound homogeneity and the high values for critical current density. For reach a high values for critical current density Jc is necessary that the polycrystalline samples microstructure to be homogeneous, which lead at one single phase necessity. The nonsuperconducting phases which appear in synthesis process must have small dimension and to be uniformly dispersed inside the material [5].

For obtaining a best quality samples it used many synthesis methods. Though generally each synthesis method have his characteristics, it exist two aspects for each other:

- all synthesis methods mix up the cations at a microscopic scale
- the requested phase it forms at high temperatures.

The most used obtaining methods for Bi:2223 polycrystalline superconductors are:

- Solid state reaction
- Coprecipitation
- Burn technique
- Liquid mix method
- Sol Gel method.

3. Experimental techniques for sample charateization

3.1. X ray diffraction

X-ray diffraction is a versatile, non-destructive analytical technique for identification and quantitative determination of the various crystalline compounds, known as “phases”, present in solid materials and powders. Identification is achieved by comparing the X-ray diffraction pattern – or “difractogram” - obtained from an unknown sample with an internationally recognized database containing reference patterns for more than 70.000 phases.

3.2. Atomic force microscopy (AFM)

Atomic force miscroscopy is a technique for the analysis of surface morphology este o tehnică de analiză a morfologiei suprafeţelor. AFM has a magnification power of up to 100 million times producing 3D images of the area studied.

3.3. Electrical resistivity

The electrical resistivity describes the normal state of oxidic superconductors, the transition region and the dissipative processes in vortex system, respectively. The change of temperature dependence of normal state resistivity of normal state resistivity from “metallic” to insulator behaviour is a source of information about the localisations processes of charge carriers (hole in Bi:22(n-1)n compounds).

3.4. A.C. magnetic susceptibilities

The AC susceptibility give information’s about the magnetization slope curve:

$$\chi = \frac{dM}{dH},$$

were M is the probe magnetisation. For this reason, the AC technique is very efficient in study of nonlinear magnetic systems, and particularly to study the inter-and intragranular processes in HTS.

4. Influence of the sintering conditions on morphology and structural and magnetic properties of Bi: 2223 polycrystalline compounds

4.1. Synthesis of (Bi, Pb): 2223 superconductors

Samples were obtained by solid state reaction of appropriate amounts of the metal oxides and carbonates of 99.99% purity. Appropriate amounts of Bi_2O_3, PbO, $SrCO_3$, BaO, $CaCO_3$, and CuO were mixed in agate mortar and calcined. The calcinated powder was pressed into pellets,7 mm diameter, and presintered at and finally sintered at different temperatures. At the end of sintering process the pellets were allowed to furnace-cool to room temperature.

The partial substitution of Bi by Pb substantially enhances the formation rate of Bi – based superconductors especially for the 2223 phase. [7]. The value of Tc depends slightly on the Pb doping amount. The partial substitution of Sr by Ba was used to induce the reduction of the modulation period.

We sintered 3 superconducting compounds systems.

4.1.1. Synthesis of superconducting compounds $(Bi_{1.8}Pb_{0.4})Sr_{1.88}Ca_2Cu_3O_y$, $(Bi_{1.6}Pb_{0.4})(Sr_{1.8}Ba_{0.2})Ca_2Cu_3O_y$

Bulk samples with nominal composition $(Bi_{1.8}Pb_{0.4})Sr_{1.88}Ca_2Cu_3O_y$ (Sample A_1) and $(Bi_{1.6}Pb_{0.4})(Sr_{1.8}\ Ba_{0.2})\ Ca_{\ 2}\ Cu_3\ O_y$ (Sample T_1 sintered at 850^0C and sample T_2 sintered at 855^0C) were obtained by the conventional solid-state reaction. [8]

These samples are presented in tabel 1.

Tabelul 1

System	Sample	Sintering temperature (^{o}C)	Compacting pressure MPa
$(Bi_{1.8}Pb_{0.4})Sr_{1.88}Ca_2Cu_3O_y$	A_1	850	p = 255
$(Bi_{1.6}Pb_{0.4})(Sr_{1.8}Ba_{0.2})Ca_2Cu_3O_y$	T_1	850	p = 255
	T_2	855	p = 255

For these samples we studied the effect of sintering temperature on structure and electrical properties.

4.1.2. Synthesis of $(Bi_{1.6}Pb_{0.4})Sr_2Ca_2Cu_3O_y$ compounds

Polycristalline bulk Bi:2223 compounds with nominal composition $(Bi_{1.6}Pb_{0.4})Sr_2Ca_2Cu_3O_y$, were obtained by the conventional solid-state reaction at the same sintering temperature by applying different uniaxial pressures (table 2).

Tabel 2

Compound	Sample	Sintering temperature (^oC)	Uniaxial pressure (MPa)
$(Bi_{1.6}Pb_{0.4})Sr_2Ca_2Cu_3O_y$	**P_1**	840	$p_1 = 100$
	P_2	840	$p_2 = 200$
	P_3	840	$p_3 = 300$
	P_4	840	$p_4 = 400$
	P_5	840	$p_5 = 500$

The effect of the uniaxial pressure on the structural and electric properties was investigated.

4.1.3.Synthesis of $(Bi_{1.6}Pb_{0.4})Sr_2BaCa_2Cu_3O_y$ and $(Bi_{1.6}Pb_{0.4})(Sr_{1.8}Ba_{0.2})Ca_2Cu_3O_y$ compounds

The $(Bi_{1.6}Pb_{0.4})Sr_2Ca_2Cu_3O_y$ and $(Bi_{1.6}Pb_{0.4})(Sr_{1.8}Ba_{0.2})Ca_2Cu_3O_y$ bulk samples are denominated **S t_n /p_n** and **Ba t_n/p_n**, respectively, where t represents the sintering temperature and p is the applied uniaxial pressure (table 3).

Tabel 3

Compound	Sample	Sintering temperature (^oC)	Uniaxial pressure (MPa)
$(Bi_{1,6}Pb_{0,4})Sr_2Ca_2Cu_3O_y$	**Proba S t1/p1**	t_1 =835	p_1= 255
	Proba S t2/p1		p_1= 255
	Proba S t2/p2		p_2= 510
	Proba S t3/p1	t_3= 845	p_1= 255
	Proba S t4/p1	t_4=850	p_1= 255
	Proba S t5/p1	t_5=852	p_1= 255
$(Bi_{1,6}Pb_{0,4})(Sr_{1,8}Ba_{0,2})Ca_2Cu_3O_y$	**Proba Ba t1/p1**	t_1=835	p_1= 255
	Proba Ba t2/p1		p_1= 255
	Proba Ba t2 /p2		p_2=510
	Proba Ba t3/p1	t_3=845	p_1= 255
	Proba Ba t4/p1	t_4=850	p_1= 255
	Proba Ba t5/p1	t_5 =852	p_1= 255

The influence of the sintering temperature and uniaxial pressure on the structural and electric properties was investigated.

In the **Ba t4/p1 samples**, (Bi,Pb)(SrBa):2223, the cooper was partially substituted by 3d transition elements like Fe and Ni, and thus $(Bi_{1.6}Pb_{0.4})(Sr_{1.8}Ba_{0.2})Ca_2(Cu_{1-x}Fe_x)_3O_y$ and $(Bi_{1.6}Pb_{0.4})(Sr_{1.8}Ba_{0.2})Ca_2(Cu_{1-x}Ni_x)_3O_y$ supraconductors with x=0.00 and x = 0.02 were obtained.

4.2. The phase purity characterization, crystalline structure and mechanical properties, as function of the sintering temperature and uniaxial pressure

4.2.1. The influence of the sintering temperature on phase purity and mechanical properties of $(Bi_{1.8}Pb_{0.4})Sr_{1.88}Ca_2Cu_3O_y$ and $(Bi_{1.6}Pb_{0.4})(Sr_{1.8}Ba_{0.2})Ca_2Cu_3O_y$ (*samples A_1, T_1 and T_2*) compounds

Figure 1 shows the X-ray diffraction patterns taken on bulk samples A_1, T_1 and T_2 . The (XRD) analysis confirmed that all samples have similar chemical composition. All the indexed reflections for sample T_2 are related to the high - Tc Bi - 2223, and with a few of peaks belonging to the “2212” and “2201” phases in A_1 and T_1 samples.

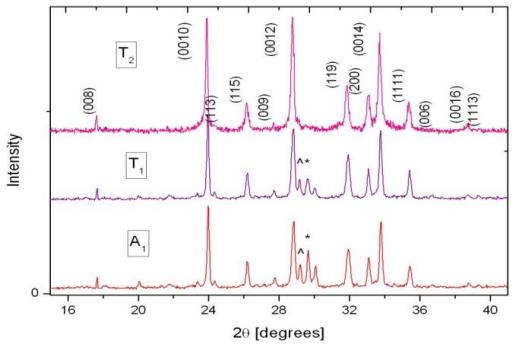

Figure 1. X-ray diffraction patterns of samples sintered at different temperatures A1, T1 and T2. The reflections belonging to the Bi-2223 phase are marked by Miller indexes , the reflections from Bi:2212 by stars(*) , and the reflections from Bi:2201 by (^).

A careful analysis of height of the X-ray diffraction patterns data indicates that the height of peaks (0010) and (0014) increases with increasing sintering temperature for sample T_2, in contrast with the decrease of the relative intensity of the peak (200). These results suggest that the increase of sintering temperature improved the grains orientation and then the texture of sample T_2.

The mechanical properties have been studied by density and Vickers with pyramidal imprint measurements. We have studied the effect of the temperature at 850^0C and 855^0C on Vickers microhardness on (Bi1.6Pb0.4)(Sr1.8Ba0.2)Ca2Cu3Oy samples.

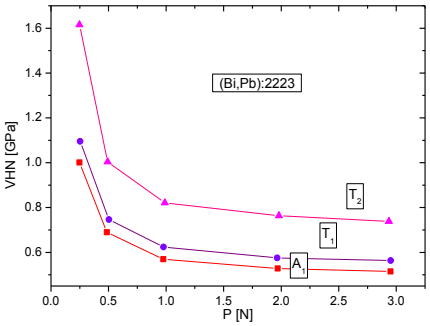

Figure 2. The variation of microhardness with applied load of samples A_1 ,T_1 and T_2.

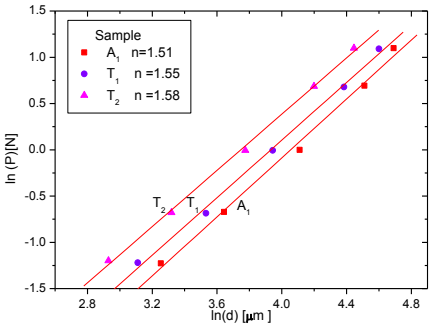

Figure 3. The applied load LnP with the Vickers diagonal Lnd for the samples A_1,T_1 and T_2.

The simplest way to describe the relationships between the applied test load ‘‘P’’ and indentation diagonal length ‘‘d’’ is Meyer’s Law (1908) [9,10]: *Log P = nlogd + log K,* where ‘‘n’’ is the Meyer number (or index) and ‘‘K’’ is the standard hardness constant. The values of Meyer’s index n are used as a measure of ISE.

In figure 3 is verified the Mayer law for A_1, T_1 and T_2. It observes the linear behaviour provided from this law and the n is modified from 1.51 to 1.58 following thermal treatment. When n < 2, the hardness increases with decreasing applied load, which is termed normal ISE. [11].

4.2.2. The influence of uniaxial pressure on the phase purity and density of $(Bi_{1.6}Pb_{0.4})Sr_2Ca_2Cu_3O_y$ compounds (P_n samples)

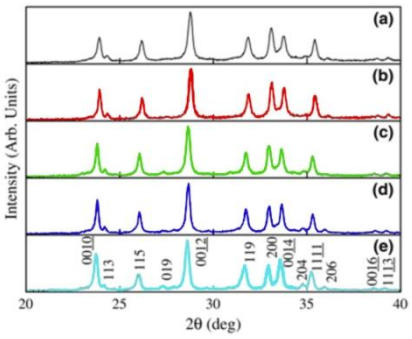

Figure 4. XRD patterns of uniaxial pressed (Bi,Pb): 2223 samples: a) 100 MPa, b) 200 MPa c) 300 MPa, d) 400 MPa, e) 500 MPa

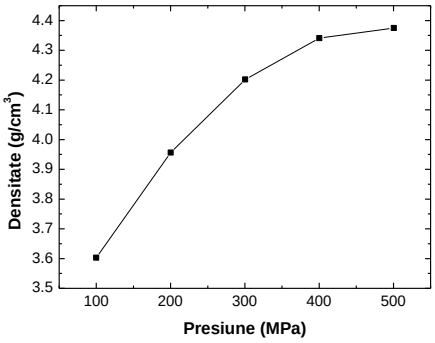

Figure 5. The influence of the applied uniaxial pressure on the densityof the (Bi, Pb):2223 samples

X-ray diffraction measurements indicate that all samples crystallize in the Bi:2223 phase. The intensity of the (00 10) and (00 14) diffraction maxima increases slightly with the applied uniaxial pressure, while the intensity of the (200) decreases. This suggests that the texture and grain orientation can be improved by applying an uniaxial pressure (mechanical deformation).

The influence of the applied uniaxial pressure in the density was investigated. Figure 5 shows the monotonic increase of the density from 3.6 g/cm^3 to 4.36 g/cm^3 with the applied uniaxial pressure.

4.2.3. Characterization of ($Bi_{1.6}Pb_{0.4}$)$Sr_2Ca_2Cu_3O_y$ compounds *(S tn/pn samples)*

The phase purity and crystal structure were analyzed by X-ray diffraction measurements.

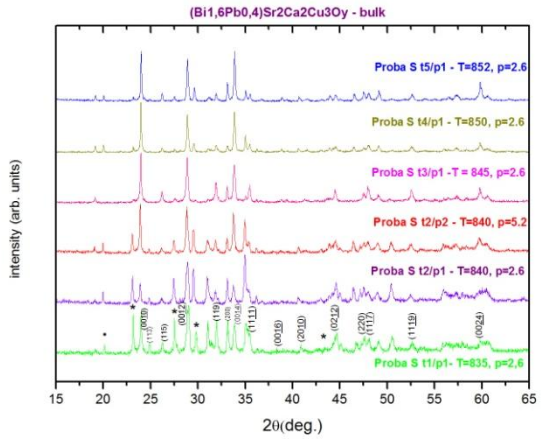

*Figure 6. XRD patterns of bulk **S samples**. The diffraction maxima of the Bi-2223 phase have Miller indices, while the ones of the Bi:2212 phase and Ca_2PbO_4 are indicated with (*) and (˙), respectively.*

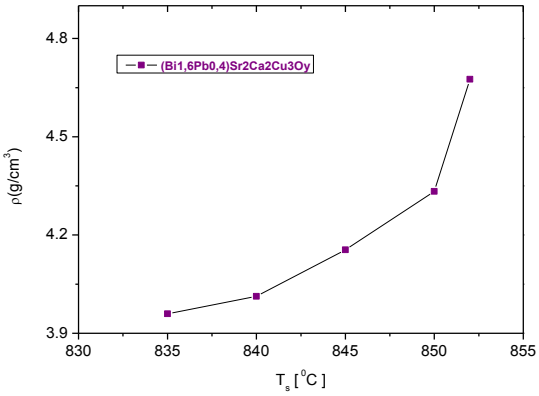

Figure 7. The sintering temperature dependence of the density for ($Bi_{1.6}Pb_{0.4}$)$Sr_2Ca_2Cu_3O_y$ obtained by applying a uniaxial pressure of 255MPa

The XRD analysis shows that in all the samples the 2223 is the majority phase and the 2212 and Ca_2PbO_4 phases are present in small proportions. With the increase of the sintering temperature the intensity of the diffraction maxima of the 2212 phase decrease. The same efect is observed by increasing the uniaxial pressure p1=255 MPa (or 2,6 t/cm^2) to p2= 510 MPa (or 5,2 t/cm^2) while keeping the sintering temperature at 840^{o}C.

Figure 7 shows that the density of the samples inceases with the sintering temperature, suggesting the improvement of crystal structure and grain orientation.

4.2.4. Characterization of $(Bi_{1.6}Pb_{0.4})(Sr_{1.8}Ba_{0.2})Ca_2Cu_3O_y$ compounds (Ba tn/pn samples)

The X-ray diffraction analysis indicates that in all samples the 2223 is the majority phase. The content of 2212 phase decreases with the increase of sintering temperature.

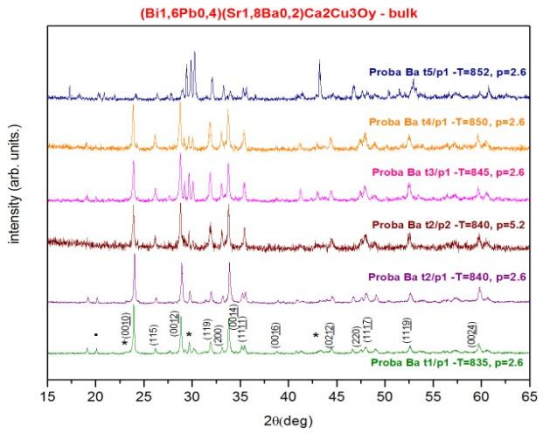

*Figure 8. XRD patterns of bulk **Ba tn/pn samples**. The diffraction maxima of the Bi-2223 phase have Miller indices, while the ones of the Bi:2212 phase are indicated with (*)*

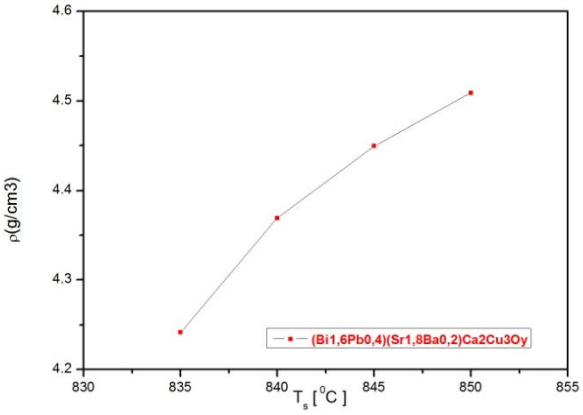

Figure 9. The sintering temperature dependence of the density for $(Bi_{1.6}Pb_{0.4})(Sr_{1.8}Ba_{0.2})Ca_2Cu_3O_y$ obtained by applying a uniaxial pressure of 255MPa

Figure 9 shows the dependence of the sintering temperature on the density of te samples. The density of the samples inceases with the sintering temperature, suggesting the improvement of crystal structure and grain orientation.

4.2.5. The influence of sintering temperature on the morphology and phase composition, studied by AFM

The AFM measurements performed in the Phase Mode on the ***S*** samples sintered at 840^{o}C and pressed at p1 = 255 MPa and p2 = 510 MPa show that the majority phase is the 2223 phase, in agreement with the X-ray diffraction analysis.

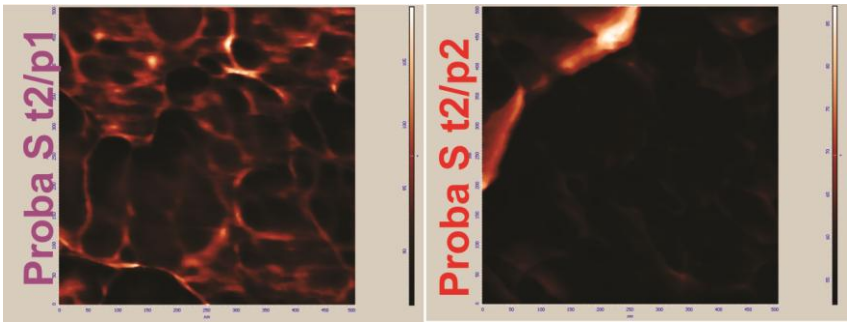

Figura 10. AFM- Phasing Mode measurements on $(Bi_{1.6}Pb_{0.4})Sr_2Ca_2Cu_3O_y$

The Tapping Mode AFM measurements indicate that the grain size increases with the increase of the applied uniaxial pressure.

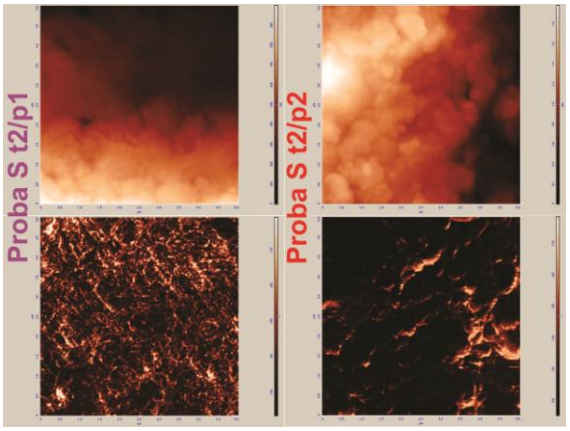

Figura 11. AFM - Tapping Mode(up)and Phasing Mode (down) measurements on $(Bi_{1.6}Pb_{0.4})Sr_2Ca_2Cu_3O_y$

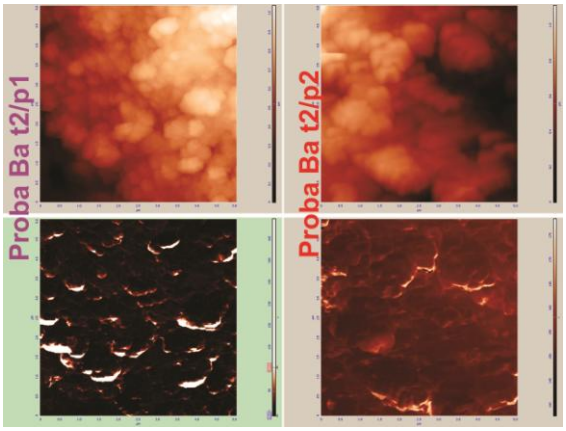

Figura 12. AFM - Tapping Mode(up)and Phasing Mode (down) measurements on $((Bi_{1.6}Pb_{0.4})(Sr_{1.8}Ba_{0.2})Ca_2Cu_3O_y$

4.3. Electrical resistivity measurements

The electrical resistivity vs. temperature measurements by four probes method A_1, T_1 and T_2 samples has been made using a Keithley 2182 nanovoltmeter and a Keithley 2400 current source. Silver paste has been used for obtaining a lowest contact resistance.

4.3.1. The temperature dependence of the electrical resistivity of $(Bi_{1.8}Pb_{0.40})Sr_{1.88}Ca_2Cu_3O_y$ (sample A_1) and $(Bi_{1.6}Pb_{0.4})(Sr_{1.8}Ba_{0.2})Ca_2Cu_3O_y$ (sample T_1 and T_2)

Figure 14 shows the temperature dependence of the electrical resistivity ρ(T) of samples A_1, T_1 and T_2.

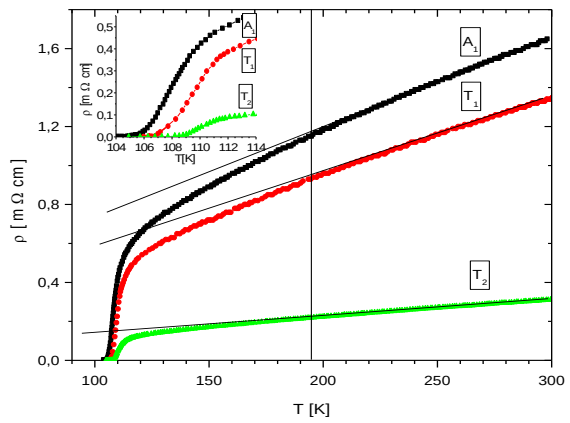

Figure 14. Temperature dependence of the electrical resistivity of samples A_1, T1 and T2. The extrapolation of linear fitting of ρ (T) curves are displayed.

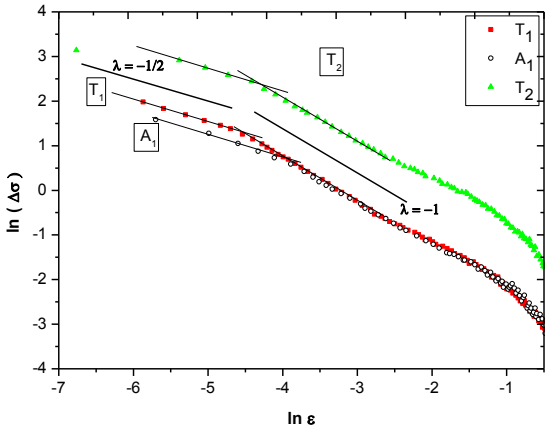

Figure 15. Determination of excess conductivity of the samples A1, T1 and T2.

The curves for T_1 and T_2 exhibit a midpoint critical transition temperature to the superconducting state T_c = 109.5 K and the curve for A_1 exhibit T_c =108K. The temperature in which the zero resistance state at sample level is observed, $T_c(\rho=0)$, increases with increasing sintering temperature (see Table 1). The $T_c(\rho=0)$ data indicate that the increase of sintering temperature result in a better connectivity between grains.

Above the excess conductivity region, in the 190K-290K temperature range, our samples are characterized by a linear temperature dependence of the electrical resistivity:

$$\rho = \rho_0 + a*T$$

where ρ_0 is the residual resistivity and a is the slope of resistivity in the normal state.

The metallic-like behavior in the normal-state region of ρ (T), suggest that the electrical current flows preferentially along the ab-plane of the oriented grains in these samples.

As shown in Table1, the ρ_0 and a parameters were influenced by the chemical composition and thermal treatments. The increase of ρ_0 suggest that the number of scattering centers increase.

In A_1 and T_1 samples, approximately the same value of p suggest for the percolative conduction, similarly transport cross sections and lengthening of conduction path. For T_2 sample, the decrease of p suggests a gradual increase of the transport current cross sections and decreasing lengthening of conduction paths with increasing sintering temperature.

On the other hand, the term ρ_{ct}, is the average intergranular electrical resistivity that is assumed to be temperature - independent, and can be obtained by utilizing the expression $\rho_{ct} = \rho(0)/p$.

Tabelul 4

Sample	T_c [K]	$T_c(\rho=0)$ [K]	$\rho(0)$ [μΩ.cm]	a=dρ/dT [μΩ.cm/K]	p	$\rho_{ct.}$ [μΩ.cm]
A1	108	105	228	4.65	6.2	37
T1	109	106.5	196	3.88	5.17	38
T2	109.5	108	50	1.27	1.7	29

Excess conductivity region starts at temperatures below $T^*=2T_c$, and ends at T_C. For a good characterization of this area experimentally measured resistivity ρ_m is compared with that extrapolated from linear dependence, ρ. At $T < T^*$ we observe $\rho_m < \rho$, so the mesured conductivity $\sigma_m = \frac{1}{\rho_m}$ is bigger that $\sigma = \frac{1}{\rho}$. Difference $\Delta\sigma = \sigma_m - \sigma > 0$ is the excess conductivity.[3]

Figure 15 shows the experimental date for the excess conductivity $\ln \Delta\sigma_0 = f(\ln \varepsilon)$. The experimental data show two linear regions with slopes around λ = -1/2, which corresponds to the 3D regime, and λ = -1, which corresponds to the 2D regime. The sample T2, obtained for the highest sintering temperature, shows the highest excess conductivity.

4.3.2. The influence of uniaxial pressure on the electrical resistivity of $(Bi_{1.6}Pb_{0.4})Sr_2Ca_2Cu_3O_y$ (P_n samples)

Figure 15 shows the effect of the uniaxial pressure on the temperature dependence of the electrical resistivity of the P_n samples belonging to $(Bi_{1.6}Pb_{0.4})Sr_2Ca_2Cu_3O_y$ superconductors. The value of the critical temperature increases slightly with the applied uniaxial pressure, probably due to the doping with free carriers. It is also expected an improvement of the intergranular contact and the orientation of the grains along the c axis with the increase of pressure.

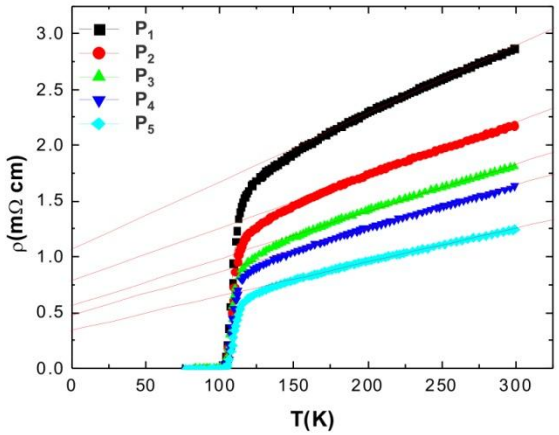

Figura 15. Temperature dependence of the resistivity for the ***P_n*** *samples obtained at 840 ^0C uniaxial pressures in the range 100 MPa - 500 MPa (probele P1-P5**).***

With the increase of uniaxial pressure the residual resistivity is reduced and the slope of the linear dependence in $\rho(T)$ decreases. This result is reflected by the decrease of the contact resistivity and of the parameter p that characterizes the percolation of the charge carriers, suggesting an improvement of the intergranular contact.

Tabel 5

Sample	Uniaxial pressure (MPa)	Critical temperature (K)	a (μΩcm/K)	ρ(0) (mΩcm)	p	ρ_{ct} (μΩcm)
P1	100	103	6.12	1.05	8.2	128
P2	200	104.5	4.73	0.72	6.3	114
P3	300	105	4.30	0.61	5.7	107
P4	400	107	3.51	0.48	4.7	102
P5	500	109	2.12	0.28	2.8	100

4.3.3. The temperature dependence of the electrical resistivity of $(Bi_{1,6}Pb_{0,4})Sr_{,2}Ca_2Cu_3O_y$ (S samples) and $(Bi_{1,6}Pb_{0,4})(Sr_{1,8}Ba_{0,2})Ca_2Cu_3O_y$ (Ba samples

Figure 16, 17, and 18 present the temperature dependence of the electrical resistivity for $(Bi_{1,6}Pb_{0,4})Sr_{,2}Ca_2Cu_3O_y$ compounds, ***S*** *samples,* and for $Bi_{1,6}Pb_{0,4})(Sr_{1,8}Ba_{0,2})Ca_2Cu_3O_y$ compounds, ***Ba*** *samples*. The shown behavior is characteristic for optimal doped samples with transitions from normal to superconductive state at temperatures below 110 K. The ρ(T) cureves show a metallic behaviour for the normal state, indicating a conduction in the ab plane.

The electrical properties of the Ba samples are improved with the increse of the sintering temperature .

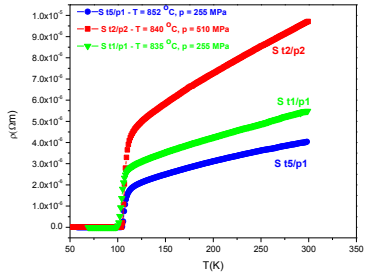

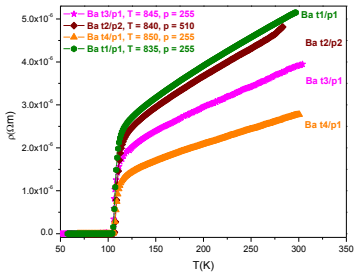

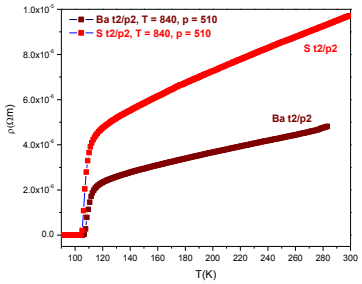

*Figure 16. The temperature dependence of the electrical resistivity for the **S** samples obtained at different sintering temperatures and uniaxial pressures*

*Figure 17. The temperature dependence of the electrical resistivity for the **Ba** samples obtained at different sintering temperatures and uniaxial pressures*

*Figure 18. The temperature dependence of the electrical resistivity for **S** and **Ba** samples obtained at the same sintering temperatures and uniaxial pressures*

The critical temperature was calculated from the maximum of dρ/dT. As presented in figures 19 and 20, the polycrystalline samples show a narrow transition from the normal to the superconductive state.

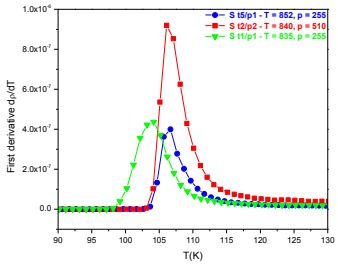

*Figure 19. The temperature dependence of dρ/dT for the **S** samples*

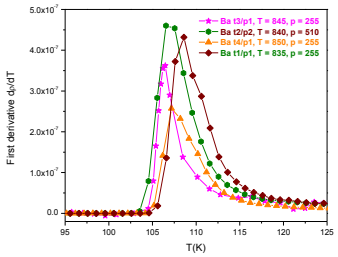

*Figure 20. The temperature dependence of dρ/dT for the **Ba** samples*

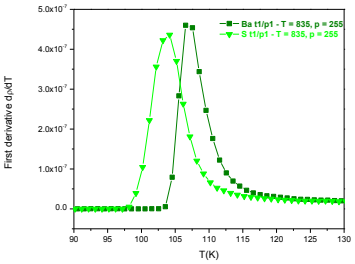

Figure 21. The temperature dependence of dρ/dT for the t1/p1 samples

The samples containing Ba show a higher transition temperature than the ***S*** samples prepared in the same conditions (Figure 21). Also the transition temeprature increases with the sintering temperature for all systems. This is an indication that the increase of sintering temperature improves the intergranular coupling.

Above $2T_C$ the temperature dependence of the electrical resistivities were fitted using a linear regression in order to obtain the residual resistivity ρ(0) and the temperature coefficient of the resistivity a=dρ/dt. The results are presented in tabels 7, 8, and 9.

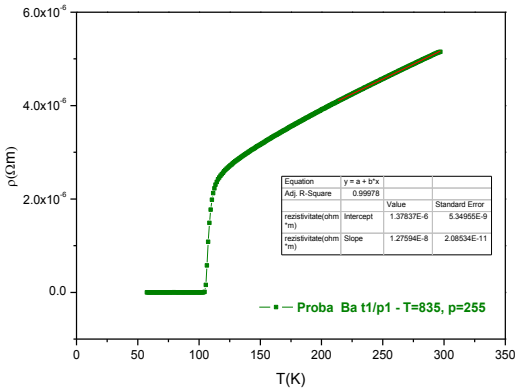

*Figura 22. The temperature dependence of the electrical resistivity for the **Ba t1/p1** sample*

Tabel 7

Sample	T_c (K)	$T_c(\rho=0)$ (K)	ΔT_c [K]	$\rho(0)$ [μΩ.cm]	a=dρ/dT [μΩ.cm/K	p	$\rho_{ct.}$ [μΩ.cm
S t1/p1	104,17	99,28	4,89	170	1,27	1,69	101
S t5/p1	106,65	104,01	2,64	129	0,97	1,29	100

Tabel 8

Sample	T_c (K)	$T_c(\rho=0)$ (K)	ΔT_c [K]	$\rho(0)$ [μΩ.cm]	a=dρ/dT [μΩ.cm/K	p	$\rho_{ct.}$ [μΩ.cm
Ba t1/p1	106,65	104,89	1,76	138	1,27	1,69	82
Ba t3/p1	106,89	105,20	1,69	98	0,98	1,31	75
Ba t4/p1	107,08	106,05	1,03	69	0,80	1,06	65

For the S tn/pn and Ba tn/pn samples both the calculated residual resistivity and temperature coefficient of the resistivity decrease with the increase of the sintering temperature, suggesting the improvement od intergranular contact. This result is reflected by the values of the p parameter that characterizes the percolation of the charge carriers.

Tabel 9

Sample	T_c (K)	$T_c(\rho=0)$ (K)	ΔT_c [K]	$\rho(0)$ [μΩ.cm]	a=dρ/dT [μΩ.cm/K	p	$\rho_{ct.}$ [μΩ.cm
S t2/p2	106,14	104,45	1,69	243	2,43	3,24	75
Ba t2/p2	108,62	106,11	2,51	99	1,33	1,77	56

Table 9 presents a direct comparison of the results for the S t2/p2 and Ba t2/p2 samples sintered in the same conditions (T = 840 ^{o}C, p = 510 MPa). The the lower values for p and ρ_{ct} suggests that Ba substitution for Sr improves the electrical properties, due to the decrease of the intergranular resistivity that influences the percolative conduction.

Figures 23, 24 and 25 present the experimental results for the excess conductivity $\ln \Delta\sigma_0 = f(\ln \varepsilon)$ for the ***S*** and ***Ba*** samples obtained at the same unxial pressure but at different sintering temperatures. The experimental data show two linear regions with slopes around λ = -1/2, which corresponds to the 3D regime, and λ = -1, which correspond to the 2D regime. The excess conductivity decreases with the increase of sintering temperature.

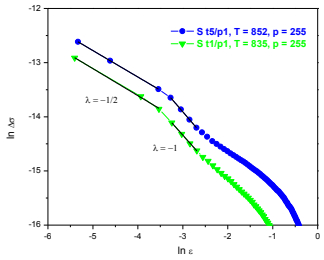

Figure 23. *The excess conductivity evaluation for S samples*

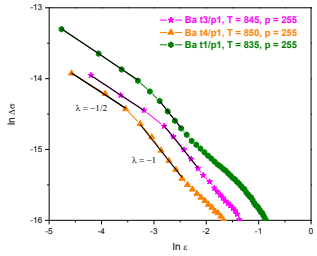

Figure 24. *The excess conductivity evaluation for Ba samples*

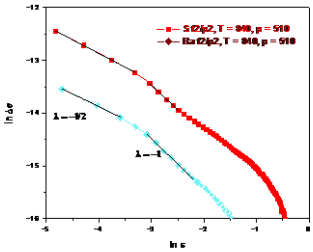

Figure 25. *The excess conductivity evaluation for St2/p2 and Ba t2/p2 samples*

5. The influence of atomic substitution on the electric and magnetic properties of Bi 2223 compounds

Bulk samples with nominal composition $(Bi_{1.6}Pb_{0.4})(Sr_{1.8}Ba_{0.2})Ca_2(Cu_{1-x}Fe_x)_3O_y$ and $(Bi_{1.6}Pb_{0.4})(Sr_{1.8}Ba_{0.2})Ca_2(Cu_{1-x}Ni_x)_3O_y$ where x=0.00 and x = 0.02, were synthesized.

5.1. Phase purity characterization by X-ray diffraction measurements

In figure 27 are presented the XRD patterns for the samples in which we made a partilly substitution of Cu with Fe, $(Bi_{1.6}Pb_{0.4})(Sr_{1.8}Ba_{0.2})Ca_2(Cu_{1-x}Fe_x)_3O_y$ where x=0.00 and x = 0.02

The XRD analysis confirmed the presence of a single “2223” phase in x = 0.00 sample. In x = 0.02 Fe sample most of the peaks belong to the “2223” phase with a few of low intensities belonging to the “2212” phase. The volume fraction of the “2223” phase obtained by using the

XRD peak intensity of (0010) in “2223”and the (008) peak intensity in “2212” was around 96% vol. for sample with x = 0.02 Fe.

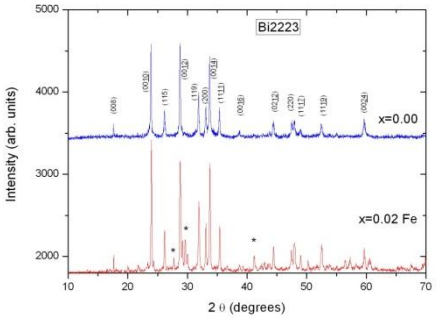

Figure 27. XRD patterns for $(Bi_{1.6}Pb_{0.4})(Sr_{1.8}Ba_{0.2})Ca_2(Cu_{1-x}Fe_x)_3O_y$ with x=0.00 and x = 0.02

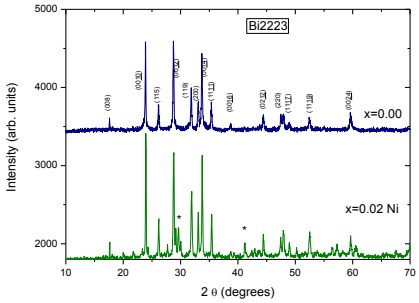

Figure 28 XRD patterns for $(Bi_{1.6}Pb_{0.4})(Sr_{1.8}Ba_{0.2})Ca_2(Cu_{1-x}Ni_x)_3O_y$ with x = 0.00 and x = 0.02

In figure 28 are presented the XRD diffraction for $(Bi_{1.6}Pb_{0.4})(Sr_{1.8}Ba_{0.2})Ca_2(Cu_{1-x}Ni_x)_3O_y$ samples with x=0.00 and x=0.02 Ni.

The XRD analysis for sample with x = 0,02 Ni shows that most of the peaks belong to the “2223” phase with a few of low intensities belonging to the “2212” phase. The volume fraction of the “2223” phase is around 95%vol.

5.2. The effects of Cu partial substitution with 3d elements on the intergranular dissipative processes by AC magnetic susceptibility measurements

The real (χ’) and imaginary (χ”) parts of the AC susceptibility were simultaneously collected with a Lake Shore Model 7000 AC susceptometer. The measurements for $\boldsymbol{(Bi_{1,6}Pb_{0,4})(Sr_{1,8}Ba_{0,2})Ca_2(Cu_{1-x}Fe_x)_3O_d}$ **(x=0.00; 0.02Fe)** samples were performed at a frequency of 1000Hz as a function of temperature at fixed AC magnetic field amplitude (Hac) in a range from 0.4 to 800 A/m.

Figure 29 shows χ’(T) behavior of real susceptibility for x=0.00 and x = 0.02 Fe sample.

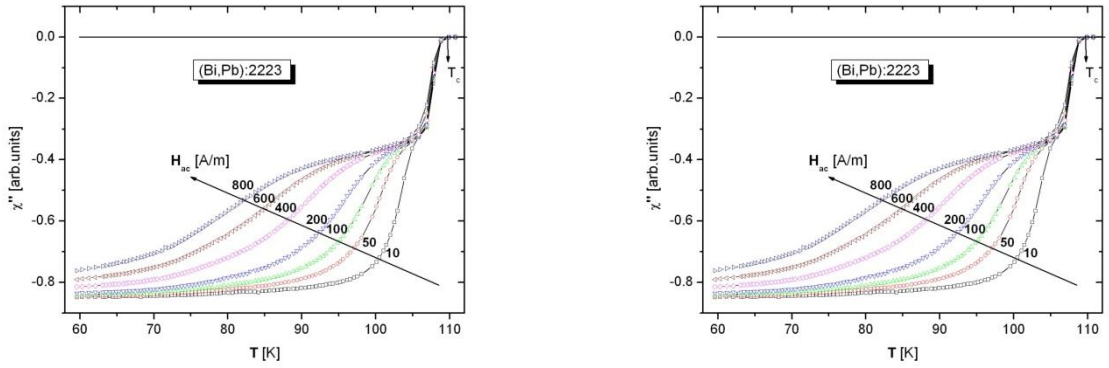

Figure 29. χ'(T) behavior of real susceptibility for x=0.00 and x = 0.02 Fe sample [8]

For x=0.00 and x=0.02 samples the real part χ'(T) show a two step behavior, characterizing the flux penetration in the intergranular matrix and in the grains respectively. The inflection point in the lower drop in the χ'(T) curve may be assigned to the intergrain critical temperature while the end of the upper step(the end of the superconductor diamagnetism) correspond to the intragrain critical temperature TCG.

The TcG values are 109,5K in x=0.00 and 99K in x=0.02 Fe .The decrease of TcG in our x=0.02 bulk samples agree with that found in Fe and Ni doped Bi:2212 single crystal. The TcG values are 109,5K for undoped sample (x=0.00) and TcG =98.5 K for x=0.02 Fe doped sample, respectively.

An important feature of HTS is the existence of „irreversibility line" (IL) where magnetic irreversibility sets in. The (IL) line is obtained from AC susceptibility measurements as a relation between the temperature Tp of the maximum in χ" (T) and the amplitude Hac of AC magnetic field.. [15]

For x=0.00 and x=0.02Fe samples, imaginary part of AC susceptibility, χ"(T), exhibit two peaks at Tp and Tg, which indicates inter-and intragranular dissipation.

For undoped sample, a small intergranular peak appear near Tg because the motion of intragrain Abrikosov vortices,and a large peak of Tp assigned to the intergranular Josephson vortices moving along the grain boundaries, respectively.

The effect of partial substitution of Cu by x=0.02 Fe, lead to the increase of intensities of the intra- and intergranular dissipation peaks (Fig.30), are shifted to temperatures lower than in x=0.00 sample.

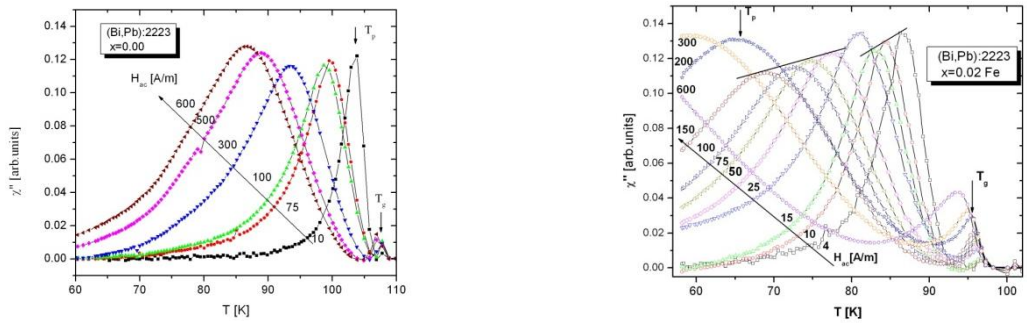

Figure 30. χ''(T) behavior of real susceptibility for x=0.00 and x = 0.02 Fe sample [8]

Figure 31 shows Tp dependence function of Hac for our samples. Above Hac= 200 A/m, for all samples, the relation Tp(Hac) seems to be linear, while a departure from this linear behavior of IL line is observed to the crossover field H*=200 A/m for x=0.00 and around H*=100 A/m for x=0.02 Fe, respectively.

As generally accepted, the irreversibility line can be described by the following power law [12,13,14]:

$$1\text{-}T_p/T_c = a\,H^q,$$

where T_c is the critical transition temperature and H the amplitude of the applied magnetic field.

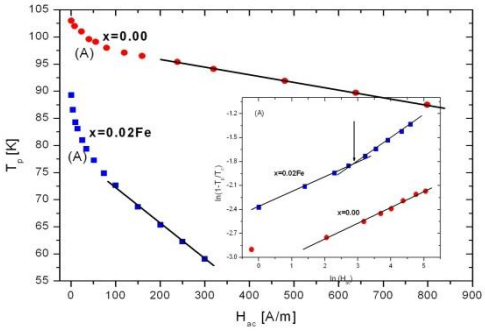

Figure 31. Intergranular χ'' –peak temperature Tp versus AC field amplitude [8]

The IL line Tp(Hac) for our samples can be divided into two regions characterized by a different behavior :a linear relation (q=1), and a nonlinear Tp(Hac) below the crossover field H*. The increase of slope a for q=1 for x=0.02 Fe (see Fig. 31), agree with the decrease of intergranular pinning force fj(0) by partial substitution of Cu by Fe. The insert of Fig. 31 shows the log-log plot of the reduced temperature t=Tp/Tc as a function of lnHac in low magnetic field.

There exists two distinct regions for the nonlinear IL, with slopes q=0.19;0.28 for x-0.02 Fe and a single region with q=0.19 for x=0.00 sample.

In conclusion the partial substitution of Cu by x = 0.02 Fe in (Bi,Pb)(Sr,Ba):2223 system leads to the decrease of Tc and shows that that -2223 phases is the majority phase.

The irreversibility line Tp(H) for the intergranular peak is found to obey the (1-Tp/Tc) = a Hq law, with a crossover from nonlinear (at low fields) to linear behavior (high fields).

Partial atomic substitution of Cu by Fe elements induced the decrease of inter- and intragranular pinning force density. [16,17]

The measurements for ***$(Bi_{1.6}Pb_{0.4})(Sr_{1.8}Ba_{0.2})Ca_2(Cu_{1-x}Ni_x)_3O_y$ (x=0.00; 0.02 Ni)*** samples were performed at a frequency of 1000Hz as a function of temperature at fixed AC magnetic field amplitude (Hac) in a range from 0.4 to 800 A/m.

Figure 32 shows χ'(T) behavior of real susceptibility for x=0.00 and x = 0.02 Ni sample.

From dependence of χ '(T) we find that the critical temperature as a result of partial substitution with x = 0.02 Ni decreases to Tc = 100 K.

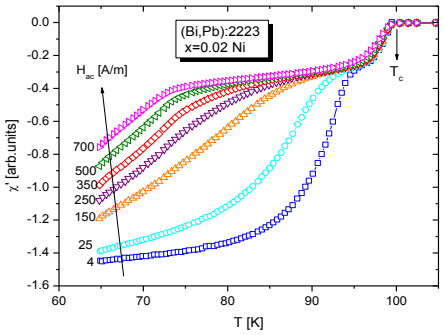

Figure 32. χ' (T) behavior of real susceptibility for x=0.00 and x = 0.02 Ni sample

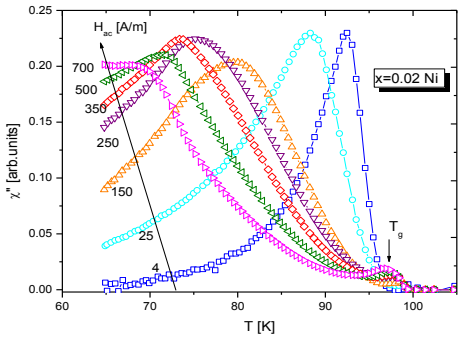

Figure 33. χ''(T) behavior of real susceptibility for x=0.00 and x = 0.02 Ni sample

For x=0.00 and x=0.02 Ni samples, imaginary part of AC susceptibility, χ"(T), exhibit two peaks at Tp and Tg, which indicates inter-and intragranular dissipation.(figure 33)

Figure 34 shows Tp dependence function of Hac for our samples.

It is noted that for samples with x = 0.00 and x = 0.02 Ni, that if magnetic field amplitude field is between the 200A / m <Hac <800A / m, Tp decrease with the increasing of Hac, following a linear law.

The increase of slope a depending on x suggest a sliht decrease of intergranular pinning force for sample with x = 0.02Ni.

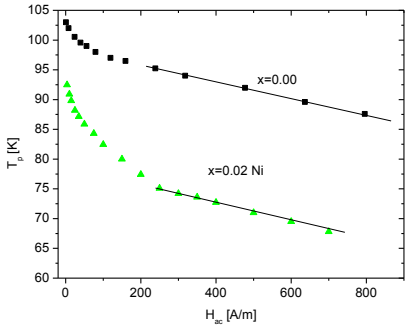

Figure 34. Tp dependence function of Hac for $(Bi_{1,6}Pb_{0,4})(Sr_{1,8}Ba_{0,2})Ca_2(Cu_{1-x}Ni_x)_3O_z$.

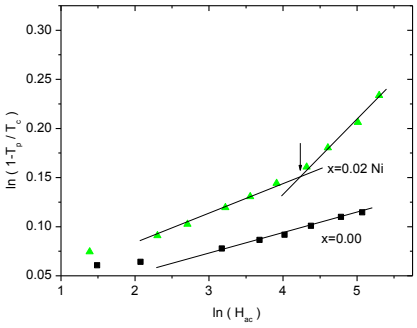

Figure 35. the log-log plot of the reduced temperature t=Tp/Tc as a function of lnHac

Figure 55 shows the log-log plot of the reduced temperature t=Tp/Tc as a function of lnHac in low magnetic field.

There exists two distinct regions for the nonlinear IL,for x = 0.02 Ni and only one for x=0.00 sample.

In conclusion the partial substitution of Cu by x = 0.02 Ni in (Bi,Pb)(Sr,Ba):2223 system:

- leads to the decrease of Tc
- The irreversibility line Tp(H) for the intergranular peak is found to obey the (1-Tp/Tc) = a Hq law, with a crossover from nonlinear (at low fields) to linear behavior (high fields).
- induced the decrease of inter- and intragranular pinning force density [18]

Selected conclusions

After the experimental investigations regarding the synthesis and characterization of the electrical and magnetic properties for the $(Bi_{1.6}Pb_{0.4})Sr_2Ca_2Cu_3O_y$, $(Bi_{1.6}Pb_{0.4})(Sr_{1.8}Ba_{0.2})Ca_2Cu_3O_y$ and $(Bi_{1.6}Pb_{0.4})(Sr_{1.8}Ba_{0.2})Ca_2(Cu_{1-x}M_x)_3O_y$ compounds where M= Fe,Ni, we reached the following conclusions:

1) The solid state reaction allows obtaining polycrystalline superconducting samples with the majority phase Bi: 2223;
2) Sintering temperature and the pressure applied for compaction the samples before sintering, along with other parameters of thermal treatment are important parameters in controlling phase purity, electric, magnetic and mechanical properties
3) By increasing the sintering temperature and compaction pressure, we obtain evidence that the volume fraction of the phase Bi: 2223 increase
4) From XRD mesurements we observed that the increase of sintering temperature improved the grains orientation and then the texture of sample
5) The density of samples increases with increasing sintering temperature differently in the two systems $(Bi_{1.6}Pb_{0.4})Sr_2Ca_2Cu_3O_y$ and (Bi1.6Pb0.4) $(Bi_{1.6}Pb_{0.4})(Sr_{1.8}Ba_{0.2})Ca_2Cu_3O_y$.
6) Vickers microhardness(VHS) on $(Bi_{1.6}Pb_{0.4})(Sr_{1.8}Ba_{0.2})Ca_2Cu_3O_y$ samples increases with increasing sintering temperature, and the relationship between applied pressure P and diagonal length of indentation d is given by Meyer's law.
7) Synthesis conditions favorised obtaining samples located in optimally doped region, or very close to it. This is confirmed by the values of critical temperatures close to 110K and narrow superconducting transition.
8) Temperature dependece of electrical resistivity shows that all samples a metallic-like behavior in the normal-state region of ρ (T), suggest that the electrical current flows preferentially along the ab-plane of the oriented grains in these samples

9) The calculated residual resistivity and temperature coefficient of the resistivity decrease with the increase of the applied uniaxial pressure, suggesting the improvement of the intergranular conduction.

10) The calculated residual resistivity and temperature coefficient of the resistivity decrease with the increase of the sintering temperature, suggesting the improvement of the intergranular contact.

11) The width of the transition from the normal to the superconductive state decreases with the increase of applied uniaxial pressure and sintering temperature, as indicated by electrical resistivity and AC magnetic measurements.

12) The partial substitution of Cu by x=0.02 Fe and Ni in $(Bi_{1.6}Pb_{0.4})(Sr_{1.8}Ba_{0.2})Ca_2Cu_3O_y$ (that showd the best superconductive properties) leads to the decrease of T_C (4K/at%) and shows that Bi:2223 phase is the majority phase.

13) The irreversibility line $Tp(H_{ac})$ for all samples can be devided into two regions characterized by different behaviors: linear (high fields) and nonlinear (at low fields) below the cross over field.

14) The linear region, at high H_{ac} (> 100A/m) can be described in the frame of the Muller model. The different slope for the doped samples indicates that Fe and Ni substitutions have different influences on the intergranular pinning force.

15) The nonlinear region for cu x=0.02 Ni/Fe shows two distinct regions, characterized by with different slopes, in the log-log plot of the reduced temperature $t=T_p/T_c$ function of lnH_{ac} pentru probele and a single region for x=0.00.

Selective references

[1] H. P. Myers, Introductory Solid State Physics 2nd Edition, Taylor & Francis, (1997)

[2] J. G. Bednorz, K. A. Müller, Z. Phys. B. 64, 189 (1986)

[3] G. Ilonca, A. V. Pop, Supraconductibilitatea şi Supraconductorii cu Temperaturi Critice Înalte, Editura BIT, Iaşi, 1998

[4] W. Meissner, R. Ochsenfeld, Natur-Wissenschaften 21, 787 (1933)

[5] A.V. Pop, D. Marconi, V. Pop, M. Pop, JOAM, Vol.8, No.2, (2006), p. 476-479

[6] Pop, A.V, Ilonca,G., Pop.M., Marconi, D., Int. J. of Mod. Phys. B, vol.18, No.15, (2004) 2169

[7] A. Pop, Introducere în fizica sistemelor vortex, Ed. Efes,Cluj-Napoca, 2004, ISBN 973-8254-62-0

[8] A. Pop, Roxana Coldea, C. Lung, Gabriela Stiufiuc, Mariana Pop, Studia Univeritatis Babes-Bolyai, Physica, LIV, 1, 2009

[9] K. Sangwal, B. Surowska, Mater. Res. Innov. 7, 91(2003)

[10] R. Tickoo, R.P. Tandon, K.K. Bamzai, P. N. Kotru, Mater. Chem. Phys. 80, 446 (2003)

[11] S.M. Khalil, A.M. Ahmed, Physica C 452, 21-28

[12] K.H.Muller and A.J.Pauza, Physica C 161, 319(1989)

[13] A.A.El-Abar, P.J.King,K.J.Maxwell,J.R.Owers-Bradley and W.B.Roys, Physica C 198,81(1992)

[14] Y.Yeshrun, A.P. Molzemoff, T.K. Worthington, R.M. Yandorfski, L. Krusin-Elbaum, F. Holtzberg, T.R. Dinger and G. Chandrasekhar, Cryogenics 29,258(1989)

[15] R. B. Flippen, T. R. Askew, J.A. Fendrich, B.M. Vleck, Physica C228, 85 (1994)

[16] A.V.Pop, D.Marconi, R. Coldea, V. Pop, Journal of Optoelectronics and Advanced Materials, Vol. 10, No. 4, p. 916-918

[17] A.V.Pop, D.Marconi, O.Anica, V.Pop, Conferinţa Internaţională „New Research Trends in Material Science" ARM-5, Sibiu, 2007, JOAM,

[18] K.H.Muller, Physica C159,717 (1989)